Octachloro- and Octabromoditechnetate(III) and Their Rhenium(III) Congeners

ARTICLE *in* INORGANIC CHEMISTRY · MARCH 2008

Impact Factor: 4.76 · DOI: 10.1021/ic701453k · Source: PubMed

4 AUTHORS, INCLUDING:

Alfred P Sattelberger
University of Nevada, Las Vegas
177 PUBLICATIONS **2,648** CITATIONS
SEE PROFILE

Steven D. Conradson
SOLEIL synchrotron
241 PUBLICATIONS **7,103** CITATIONS
SEE PROFILE

Ken Czerwinski
University of Nevada, Las Vegas
232 PUBLICATIONS **1,583** CITATIONS
SEE PROFILE

Inorg. Chem. **2008**, *47*, 1991−1999

Octachloro- and Octabromoditechnetate(III) and Their Rhenium(III) Congeners

Frederic Poineau,*,† Alfred P. Sattelberger,†,‡,§ Steven D. Conradson,§ and Kenneth R. Czerwinski†

Harry Reid Center for Environmental Studies, University of Nevada Las Vegas, Las Vegas, Nevada 89154, Physical Sciences Directorate, Argonne National Laboratory, 9700 Cass Avenue, Lemont, Illinois 60439, and Materials Physics Division, Los Alamos National Laboratory, P.O. Box 1663, Los Alamos, New Mexico 87545

Received July 22, 2007

The compound $(n\text{-}Bu_4N)_2Tc_2Br_8$ was prepared by the metathesis of $(n\text{-}Bu_4N)_2Tc_2Cl_8$ with HBr (g) in dichloromethane and characterized by X-ray absorption fine structure spectroscopy and UV–vis spectroscopy. Analysis of the data gives a Tc−Tc distance of 2.16(1) Å and a Tc−Br distance of 2.48(1) Å. The Tc(III) oxidation state was inferred by the position of the edge absorption, which reveals a shift of 12 eV between $(n\text{-}Bu_4N)_2Tc_2Br_8$ and NH_4TcO_4. The analogous shift between $(n\text{-}Bu_4N)_2Tc_2Cl_8$ and NH_4TcO_4 is 11 eV. The UV–vis spectrum of $Tc_2Br_8^{2-}$ in dichloromethane exhibits the characteristic $\delta \rightarrow \delta^*$ transition at 13 717 cm^{-1}. The $M_2X_8^{2-}$ (M = Re, Tc; X = Cl, Br) UV–vis spectra are compared, and the position of the $\delta \rightarrow \delta^*$ transition discussed.

Introduction

Technetium, element 43, occupies a central position in the periodic table. It is the lowest-atomic-number radioelement, and 34 unstable isotopes of the element are known with mass numbers ranging from 85 to 118. The most readily available isotope is ^{99}Tc ($t_{1/2} = 2.1 \times 10^5$ years, $\beta_{max} = 292$ keV), which is isolated in large quantities from spent nuclear fuel, where it constitutes approximately 6% of the fission yield (*via* ^{99}Mo). The coordination chemistry of technetium, spanning oxidation states from +7 to −1, is similar to but not nearly as extensive as that of its heavier congener rhenium. In their lower oxidation states, both metals have a tendency to polymerize and form complexes with metal−metal bonds. The radioactive nature of technetium and the associated costs of radiological laboratories and waste disposal explain why its chemistry has not developed to the extent of its Re congener. At the Harry Reid Center for Environmental Studies on the UNLV campus, we have developed the capability to work with macro quantities of technetium and to explore the synthetic and structural chemistry of this fascinating element.

The octahalodirhenate ions, $Re_2X_8^{2-}$ (X = Cl, Br), are archetypal quadruply metal−metal-bonded complexes and have been well studied both from a spectroscopic point of view and as precursors to other quadruply bonded Re(III) dimers. Their technetium(III) analogues, $Tc_2X_8^{2-}$ (X = Cl, Br), are less well-known and their chemistry relatively unexplored.[1] The compound $(n\text{-}Bu_4N)_2Tc_2Cl_8$ is a potential precursor to many other multiply bonded technetium dimers. It has been claimed by several different laboratories using different synthetic methods, but its preparation in pure form has proven difficult and in some instances has been controversial.[2–4,8] The chloro dimer, isostructural with $(n\text{-}Bu_4N)_2Re_2Cl_8$, has been characterized by single-crystal X-ray diffraction, IR, Raman, UV–vis spectroscopy, electrochemistry, and density functional theory (DFT) calculations.[2–7] The compound $(n\text{-}Bu_4N)_2Tc_2Br_8$ was reported in 1980; it was obtained when a solution of $(n\text{-}Bu_4N)_2Tc_2Cl_8$ in acetone was

* Author to whom correspondence should be addressed. E-mail: freder29@unlv.nevada.edu.
† University of Nevada Las Vegas.
‡ Argonne National Laboratory.
§ Los Alamos National Laboratory.

(1) Sattelberger, A. P. *Multiple Bonds between Metal Atoms*, 3rd ed.; Cotton, F. A., Murillo, C. A., Walton, R. A. , Eds.; Springer: New York, 2005.
(2) Cotton, F. A.; Daniels, L.; Davison, A.; Orvig, C. *Inorg. Chem.* **1981**, *20*, 3051–3055.
(3) Schwochau, K.; Hedwig, K.; Schenk, H. J.; Greis, O. *Inorg. Nucl. Chem. Lett.* **1977**, *13*, 77–80.
(4) Preetz, W.; Peters, G. *Z. Naturforsch., B: Chem. Sci.* **1980**, *35*, 797–801.
(5) Cotton, F. A.; Pedersen, E. *Inorg. Chem.* **1975**, *14*, 383–387.
(6) Cavigliasso, G.; Kaltsoyannis, N. *Dalton Trans.* **2006**, *46*, 5476–5483.
(7) Cavigliasso, G.; Kaltsoyannis, N. *Inorg. Chem.* **2007**, *46*, 3557–3565.
(8) Preetz, W.; Peters, G.; Bublitz, D. *J. Cluster Sci.* **1994**, *5*, 83–106.

10.1021/ic701453k CCC: $40.75
Published on Web 02/22/2008

treated with hydrobromic acid and evaporated to dryness. The resulting carmine red compound was characterized by IR, Raman, and chemical analysis, but no structural data were reported.[4] Estimates of key structural parameters were made on the basis of Raman measurements[8] and more recently by DFT calculations.[6,7] Both compounds are diamagnetic d^4-d^4 dimers with quadruple metal−metal bonds. They are stable in the solid state and reasonably stable in organic solvents (e.g., acetone and dichloromethane) under anaerobic conditions. In cases where X-ray-quality single crystals cannot be isolated, X-ray absorption fine structure spectroscopy (XAFS) has proven itself as a powerful technique for the determination of oxidation states and structural parameters, and it has been applied successfully to several multiply bonded technetium[9,10] and rhenium dimers.[11] The goals of the present study were to reinvestigate the methods used for the synthesis of $(n\text{-}Bu_4N)_2Tc_2X_8$, to optimize a set of procedures, to determine structural parameters for $Tc_2Br_8^{2-}$, and to measure and compare the electronic spectra of the $Tc_2X_8^{2-}$ and $Re_2X_8^{2-}$ systems.

Experimental Section

Caution! *Techetium-99 is a weak β emitter (E_{max} = 292 keV). All manipulations were performed in a laboratory designed for radioactivity using efficient HEPA-filtered fume hoods and Schlenk and glovebox techniques and following locally approved radiochemistry handling and monitoring procedures. Laboratory coats, disposable gloves, and protective eyewear were worn at all times.*

NH_4TcO_4 was purchased from Oak Ridge National Laboratory. The compound, which should be pure white, contains a black impurity; prior to use, it was purified and converted to $(n\text{-}Bu_4N)TcO_4$ (see below). The solvents and reagents (THF, acetone, ether, $(n\text{-}Bu_4N)BH_4$, $(n\text{-}Bu_4N)HSO_4$, CH_2Cl_2, hexane, and 12 M HCl) were purchased from Sigma/Aldrich and used as received. A lecture bottle of HBr (g) was purchased from Matheson and used as received. $(n\text{-}Bu_4N)_2Re_2X_8$ (X = Cl, Br) were synthesized according to the method described by Cotton and co-workers.[12]

Preparation of $(n\text{-}Bu_4N)TcO_4$. A 0.844 g sample of impure NH_4TcO_4 was dissolved/suspended in 15 mL of deionized water in a 100 mL round-bottom flask, and 30 μL of 30% aqueous hydrogen peroxide and 50 μL of concentrated NH_4OH were added to the black suspension. The flask was placed on a rotary evaporator and heated for 1 h while rotating in a 100 °C oil bath. The hot oil bath was removed, the solution was allowed to cool to ca. 80 °C, and the clear, colorless solution was then *carefully* evaporated to dryness under a vacuum. After drying, the NH_4TcO_4 in the 100 mL flask was dissolved in 10 mL of water and the solution was carefully transferred by disposable pipet to a 50 mL centrifuge tube. Then, 1.5 g of $(n\text{-}Bu_4N)HSO_4$ dissolved in 10 mL of deionized water was added dropwise, and voluminous white $(n\text{-}Bu_4N)TcO_4$ precipitated. The suspension was centrifuged, the supernate was removed with a disposable glass pipet, and the solid was washed with 20 mL of ice-cold water. After drying over Drierite for 24 h in a desiccator, 1.610 g (3.965 mmol) of a fluffy white solid was recovered, yield, 85.2%.

Preparation of $(n\text{-}Bu_4N)_2Tc_2Br_8$. The compound was synthesized by a modification of the procedure reported by Preetz and co-workers.[8] The synthesis has three stages: (1) reduction of $(n\text{-}Bu_4N)TcO_4$ to $(n\text{-}Bu_4N)TcOCl_4$, (2) reduction of $(n\text{-}Bu_4N)TcOCl_4$ to $(n\text{-}Bu_4N)_2Tc_2Cl_8$, and (3) conversion of $(n\text{-}Bu_4N)_2Tc_2Cl_8$ to $(n\text{-}Bu_4N)_2Tc_2Br_8$.

1. Synthesis of $(n\text{-}Bu_4N)TcOCl_4$. A total of 30 mL of 12 M HCl was added to the 1.610 g (3.965 mmol) of $(n\text{-}Bu_4N)TcO_4$ from the previous step, a small magnetic stir bar was added, and the suspension was stirred for 30 min at room temperature. Voluminous green $(n\text{-}Bu_4N)TcOCl_4$ precipitated. The compound was centrifuged, and the supernate was removed and discarded. The solid treated a second time with 30 mL of fresh, cold (5 °C) concentrated HCl for 30 min. After centrifugation, the clear supernate was decanted, and the green $(n\text{-}Bu_4N)TcOCl_4$ was thoroughly dried in a vacuum desiccator overnight. The solid was recrystallized from a mixture of (minimal) acetone/ether, and 1.607 g was obtained (3.214 mmol): yield, 81%.

2. Synthesis of $(n\text{-}Bu_4N)_2Tc_2Cl_8$. The reaction was performed in a 250 mL round-bottom flask equipped with three-hole rubber stopper. A 1.439 g (2.878 mmol) portion of $(n\text{-}Bu_4N)TcOCl_4$ was dissolved in 30 mL of THF. The solution was purged for 10 min with Ar using a disposable pipet. A solution of $(n\text{-}Bu_4N)BH_4$ (1.493 g, 5.80 mmol) in 50 mL of THF was then carefully added dropwise under Ar over the course of 20 min. A change of color from bright green to brown and effervescence were observed during the addition. Ten minutes after the addition, 100 mL of air-free ether was added slowly to the solution. The argon bubbling was stopped; the flask was closed with a rubber septum. A brown oil was observed at the bottom of the flask. After 30 min, the ether was removed by pipet, and the oil was then pumped to dryness under a vacuum (<0.1 torr). (N.B., if the brown product is not completely dry, the yield of the product in the next step drops considerably.)

The brown powder obtained from the previous step was dissolved with stirring in 20 mL of acetone under air. After 2 min, the solid was completely dissolved, then 1 mL of concentrated HCl was slowly added dropwise with stirring (∼5 min). The solution turned from brown to green. After another 5 min, 30 mL of precooled (5 °C) ether was slowly added to the stirred solution. After 3 min, a green precipitate appeared, and the solution was stored for 8 h at −25 °C in a freezer. The brown supernate was removed, and the green/brown solid was washed with 1.5 mL of acetone. The resulting emerald green solid was recrystallized two times from minimal CH_2Cl_2/hexane. A yield of 0.885 g (0.929 mmol) of $(n\text{-}Bu_4N)_2Tc_2Cl_8$ was obtained (64.6%). The compound was characterized by UV–vis, XAFS spectroscopy, and powder X-ray diffraction (XRD).

3. Synthesis of $(n\text{-}Bu_4N)_2Tc_2Br_8$. A 0.150 g (0.157 mmol) sample of $(n\text{-}Bu_4N)_2Tc_2Cl_8$ was dissolved in 15 mL of dichloromethane in a 100 mL round-bottom flask and purged with argon through a disposable pipet. The solution was warmed to 30 °C in an oil bath. A stream of gaseous HBr was then simultaneously passed through the solution, which turns from green to red. After 15 min, the flow of HBr was halted and the solution evaporated to dryness with the argon stream. The red solid was dissolved in minimal boiling dichloromethane and then cooled to −25 °C in a freezer; 0.138 g (0.103 mmol) of microcrystalline $(n\text{-}Bu_4N)_2Tc_2Br_8$ was obtained (65.6%) after removal of the supernate and drying under a vacuum. The UV–vis spectrum of $Tc_2Br_8^{2-}$ was recorded in degassed dichloromethane. The compound oxidizes relatively

(9) Almahamid, I.; Bryan, J. C.; Bucher, J. J.; Burrell, A. K.; Edelstein, N. M.; Hudson, E. A.; Kaltsoyannis, N.; Lukens, W. W.; Shuh, D. K.; Nitsche, H.; Reich, T. *Inorg. Chem.* **1995**, *34*, 193–198.
(10) Allen, P. G.; Siemering, G. S.; Shuh, D. K.; Bucher, J. J.; Edelstein, N. M.; Langton, C. A.; Clark, S. B.; Reich, T.; Denecke, M. A. *Radiochim. Acta* **1997**, *76*, 77–86.
(11) Conradson, S. D.; Sattelberger, A. P.; Woodruff, W. H. *J. Am. Chem. Soc.* **1988**, *110*, 1309–1311.
(12) Cotton, F. A.; Curtis, N. F.; Johnson, B. F.; Robinson, W. R. *Inorg. Chem.* **1965**, *4*, 326–330.

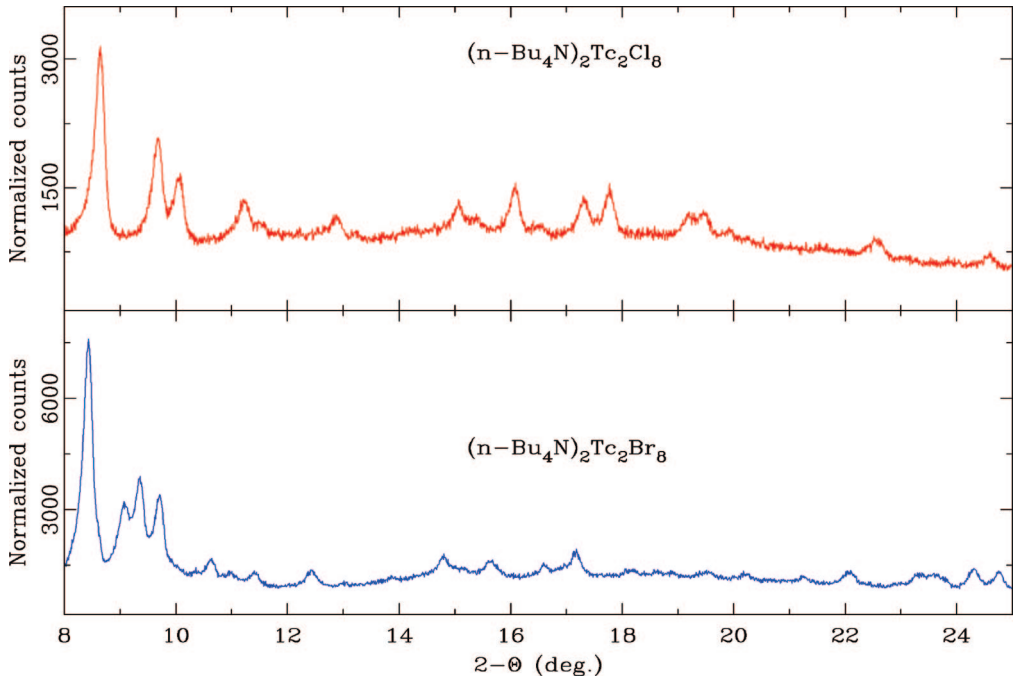

Figure 1. X-ray diffraction powder patterns of $(n\text{-}Bu_4N)_2Tc_2Cl_8$ and $(n\text{-}Bu_4N)_2Tc_2Br_8$ used in the XAFS studies.

quickly in solution if exposed to air. This compound was characterized by UV–vis, XAFS spectroscopy, and powder XRD.

X-Ray Absorption Fine Structure Spectroscopy. XAFS measurements were performed at the Stanford Synchrotron Radiation Laboratory, under dedicated operating conditions (3.0 GeV, 50–100 mA), on end station 11-2. The samples were prepared by dilution of the Tc compounds (NH_4TcO_4, $(n\text{-}Bu_4N)TcOCl_4$, $(n\text{-}Bu_4N)_2Tc_2Cl_8$, and $(n\text{-}Bu_4N)_2Tc_2Br_8$) in boron nitride and placed in slots in an aluminum sample folder with Kapton windows. Sample holders were attached to the coldfinger of a liquid N_2 cryostat so that the sample temperatures were near 80 K. Si [220] crystals were used to monochromate the beam. Harmonics were eliminated with a flat, Pt-coated mirror tilted to a cutoff energy of ca. 25 keV. All spectra were recorded between $k = 0$ and 14 $Å^{-1}$ in both transmission and fluorescence mode using a multielement Ge detector and digital amplifiers.

A dead time correction of around 1 μs was made to adjust the absorption peak height to match that of the transmission data. This procedure can also correct for self-absorption. Energy calibration was accomplished by measuring the spectrum of a Tc foil with a third ion chamber (edge energies). The first inflection point of the Tc foil was defined as 21 044.0 eV. The extended X-ray absorption fine structure (EXAFS) was extracted from the spectra using Autobk software, which minimizes R space values in low k space. Data analysis was performed using Winxas. The resulting EXAFS spectra were k^2-weighted, and Fourier transform was performed between $k = 3.7$ and 13.7 $Å^{-1}$. For the fitting procedure, the amplitude and phase-shift function were calculated by Feff8.2. Input files were generated by Atoms using crystallographic structures of $(n\text{-}Bu_4N)_2Tc_2Cl_8$ and $(n\text{-}Bu_4N)_2Re_2Br_8$.[2,13] Adjustments of the k^2-weighted EXAFS spectra were performed under the constraints $S_0^2 = 0.9$. During the fitting procedure, the energy shift parameter (ΔE_0) was constrained to the same value for all scattering.

Other Techniques. ^{99}Tc concentrations were determined by liquid scintillation counting using a Packard 2500 scintillation analyzer. The scintillation cocktail was ULTIMA GOLD AB (Packard). UV–visible spectra were recorded at room temperature in dichloromethane in a quartz cell (1 cm) on a Cary 6000i double-beam spectrometer with a dichloromethane reference. For XRD measurements, the samples ($m \sim 5$ mg) were mixed with a standard (Silicon SRM 640c) placed on a silicon disk, covered with Kapton foil, and placed in the instrument for measurement. The XRD patterns were obtained using a Philips PANalytical X'Pert Pro instrument with a Cu Kα target and a Ni filter. Lattice parameters were refined using the GSAS software package.

(13) Huang, H. W.; Martin, D. S. *Inorg. Chem.* **1985**, *24*, 96–101.

Table 1. Crystallographic Parameters for $(n\text{-}Bu_4N)_2Tc_2X_8$ (X = Cl, Br) Determined Experimentally and Comparison with Literature Data

	compounds			
lattice parameter (Å) and angle (deg)	$(n\text{-}Bu_4N)_2Tc_2Cl_8$ [this work]	$(n\text{-}Bu_4N)_2Tc_2Cl_8$ [ref 2]	$(n\text{-}Bu_4N)_2Tc_2Br_8$ [this work]	$(n\text{-}Bu_4N)_2Re_2Br_8$ [13]
a	10.973(1)	10.915(1)	14.571(1)	14.328(3)
b	15.642(1)	15.382(1)	15.640(1)	15.503(3)
c	16.572(1)	16.409(1)	11.423(1)	11.381(3)
β	121.98(1)	122.37(1)	97.83(1)	97.10(1)

Results

Powder X-Ray Diffraction. $(n\text{-}Bu_4N)_2Tc_2Cl_8$. Analysis of the XRD powder patterns of the sample used for the EXAFS study (Figure 1) confirm the presence of $(n\text{-}Bu_4N)_2Tc_2Cl_8$ as a single phase without impurities. The XRD powder pattern was indexed with the monoclinic cell found in the literature[2] and the lattice parameters subsequently refined (Table 1) with Si powder as an internal standard.

$(n\text{-}Bu_4N)_2Tc_2Br_8$. Analysis of the XRD powder patterns (Figure 1) indicates that the $(n\text{-}Bu_4N)_2Tc_2Br_8$ sample does not contain any residual $(n\text{-}Bu_4N)_2Tc_2Cl_8$. Since it is expected that $(n\text{-}Bu_4N)_2Re_2Br_8$ will have a similar lattice, the XRD powder pattern of $(n\text{-}Bu_4N)_2Tc_2Br_8$ was mainly indexed with the monoclinic cell of the Re congener.[13] The cell parameters

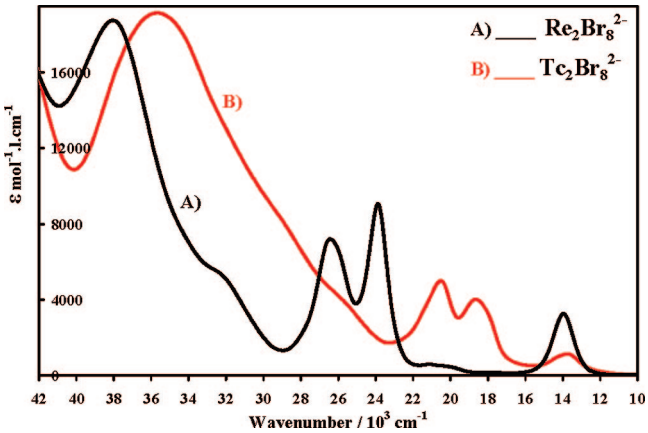

Figure 2. Absorption spectra of $Tc_2Br_8^{2-}$ (B, red) and $Re_2Br_8^{2-}$ (A, black) in dichloromethane.

Table 2. Wavenumber (cm^{-1}) and Absorption Coefficient (M^{-1} cm^{-1}) determined for $M_2X_8^{2-}$ (M = Tc, Re; X = Cl, Br) in Dichloromethane

compound	ν, cm^{-1} (ϵ, M^{-1} cm^{-1})
$Tc_2Cl_8^{2-}$	14713 (1391); 25623 (8674); 33016 (10564)
$Tc_2Br_8^{2-}$	13717 (1147); 18647 (4019); 20518 (5007); 35714 (18145)
$Re_2Cl_8^{2-}$	14589 (2556); 32003 (11430); 39447 (10742)
$Re_2Br_8^{2-}$	13957 (3268); 23879 (9061); 26430 (7212); 38022 (18742)

of $(n\text{-}Bu_4N)_2Tc_2Br_8$ were subsequently refined (Table 1) with Si powder as an internal standard.

UV–Visible Spectroscopy. $M_2Br_8^{2-}$. The rhenium(III) and technetium(III) bromide dimers were dissolved in dichloromethane, and the spectra were recorded between 50 000 and 5 000 cm^{-1} (Figure 2). The spectrum of $Tc_2Br_8^{2-}$ exhibits four intense bands at 13 717, 18 647, 20 518, and 35 714 cm^{-1}. The extinction coefficients of these bands are presented in Table 2. Examination of the spectrum in the vicinity of 22 500 cm^{-1} reveals the absence of $TcBr_6^{2-}$.[14] The lowest energy transition for $Tc_2Br_8^{2-}$ is logically assigned as the $\delta \rightarrow \delta^*$ transition. The spectrum of $Re_2Br_8^{2-}$ is similar to that reported in the literature and exhibits four intense bands at 13 957, 23 879, 26 430, and 38 022 cm^{-1}. The band at 13 957 cm^{-1} has been assigned as the $\delta \rightarrow \delta^*$ transition.[15]

The spectra of $Tc_2Br_8^{2-}$ and $Re_2Br_8^{2-}$ exhibit similar features with the presence of four intense absorption bands. The bands at the lowest energy (13 717 cm^{-1} for M = Tc and 13 957 cm^{-1} for M = Re) are nearly superimposable, while the other bands are shifted to higher energy for the Re compound. The bands are narrower with higher intensities for $Re_2Br_8^{2-}$. The extinction coefficient for the $Re_2Br_8^{2-}$ $\delta \rightarrow \delta^*$ transition is 2.85 times larger than that for $Tc_2Br_8^{2-}$, and the full width at half-maximum is 1310 versus 2120 cm^{-1}.

$M_2Cl_8^{2-}$. The spectrum of $Tc_2Cl_8^{2-}$ (Figure 3) is identical to that reported in the literature showing the characteristic $\delta \rightarrow \delta^*$ transition at 14 713 cm^{-1}.[2–4] Our measured extinction coefficient (Table 2) for this transition is close to that reported.[2] No oxidation of $Tc_2Cl_8^{2-}$ is observed, consistent with the lack of the $TcCl_6^{2-}$ absorbance at 29 500 cm^{-1}.[16]

(14) Colin, M.; Ianovici, E.; Lerch, P. *J. Radioanal. Nucl. Chem.* **1988**, *120*, 175–183.
(15) Clark, R. J.; Stead, M. J. *Inorg. Chem.* **1983**, *22*, 1214–1220.
(16) Kanchiku, Y. *Bull. Chem. Soc. Jpn* **1969**, *42*, 2831–2835.

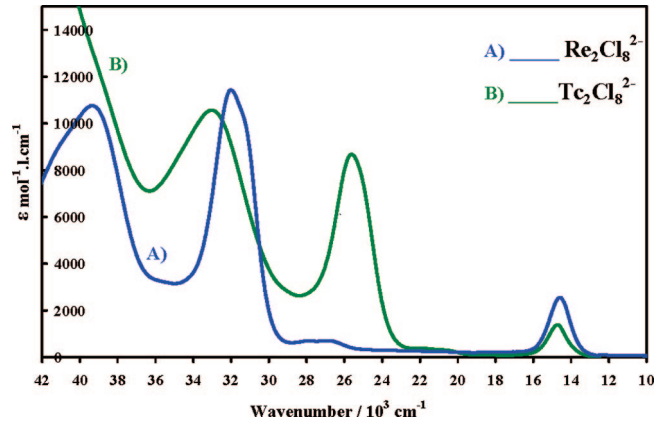

Figure 3. Absorption spectra of $Tc_2Cl_8^{2-}$ (B, green) and $Re_2Cl_8^{2-}$ (A, blue) in dichloromethane.

Table 3. Wavenumber (cm^{-1}) and Absorption Coefficient (M^{-1} cm^{-1}) of the $\delta \rightarrow \delta^*$ Transition Determined for $Re_2Cl_8^{2-}$ in Methanol, Acetonitrile, Acetone, and Dichloromethane

solvent	ν, cm^{-1} (ϵ, M^{-1} cm^{-1})
methanol[12]	14500 (1530)
acetonitrile[12]	14700 (2340)
acetone[12]	14700 (2480)
dichloromethane	14589 (2556)

The spectrum of $Re_2Cl_8^{2-}$ recorded in dichloromethane is similar to the spectra measured previously in methanol, acetonitrile, and acetone.[12] The band at 14 589 cm^{-1} is assigned as the $\delta \rightarrow \delta^*$ transition.[15] The exact position and extinction coefficient of the $\delta \rightarrow \delta^*$ transition are a function of the solvent (Table 3).[12] The spectra of $Re_2Cl_8^{2-}$ and $Tc_2Cl_8^{2-}$ exhibit similar features with the presence of three major absorption bands. As for $(n\text{-}Bu_4N)_2M_2Br_8$ (M = Re, Tc), the $\delta \rightarrow \delta^*$ transitions (14 713 cm^{-1} for M = Tc and 14 589 cm^{-1} for M = Re) are nearly superimposable, while the other bands are shifted to higher energy for the Re compound.

XAFS Spectroscopy. XANES. The XANES spectra of $(n\text{-}Bu_4N)TcOCl_4$, $(n\text{-}Bu_4N)_2Tc_2X_8$ (X = Cl, Br), and NH_4TcO_4 (Figure 4) were recorded, and the background was subtracted and normalized. XANES spectroscopy is commonly used for characterization of the local geometry and oxidation state of absorbing atoms. Previous studies showed that the Tc K-edge position can be correlated to the oxidation state of the absorbing atom and that Tc species with tetrahedral and square pyramidal geometry exhibit a pre-edge feature in their XANES spectra.[9,10] The XANES spectra reveal a pre-edge for NH_4TcO_4 and for $(n\text{-}Bu_4N)TcOCl_4$, which is characteristic of the electronic transition s → p in the tetrahedral (TcO_4^-) and square pyramidal ($TcOCl_4^-$) geometries. In the XANES of $Tc_2X_8^{2-}$ (X = Cl, Br), no pre-edge features were observed. In these compounds, the first unoccupied molecular orbital (MO) has δ symmetry and the s → d transition is forbidden. Analysis of the absorption edge position indicates that the shift to lower energy observed in the series TcO_4^-, $TcOCl_4^-$, $Tc_2Cl_8^{2-}$, and $Tc_2Br_8^{2-}$ is consistent with the decrease in oxidation state of the Tc atom (Table 4). The absences of a pre-edge in the XANES spectra of $Tc_2X_8^{2-}$ (from unreacted $TcOCl_4^-$ or TcO_4^-), and the position of the absorption edge, in accordance with Tc(III),

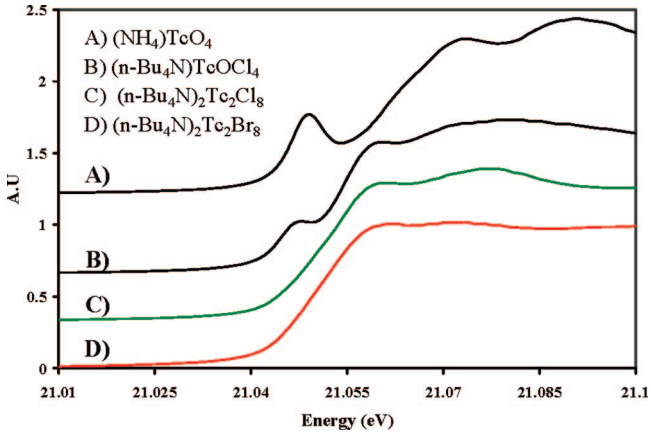

Figure 4. Normalized Tc−K edge spectra of (A) NH_4TcO_4, (B) $(n\text{-}Bu_4N)TcOCl_4$, (C) $(n\text{-}Bu_4N)_2Tc_2Cl_8$, and (D) $(n\text{-}Bu_4N)_2Tc_2Br_8$.

Table 4. Position of Tc−K edge absorption of NH_4TcO_4, $(n\text{-}Bu_4N)TcOCl_4$, $(n\text{-}Bu_4N)_2Tc_2Cl_8$, and $(n\text{-}Bu_4N)_2Tc_2Br_8$

compound	edge absorption (eV)
NH_4TcO_4	21063
$(n\text{-}Bu_4N)TcOCl_4$	21055
$(n\text{-}Bu_4N)_2Tc_2Cl_8$	21052
$(n\text{-}Bu_4N)_2Tc_2Br_8$	21051

Table 5. Main Scattering Calculated in $Tc_2X_8^{2-}$ (X = Cl, Br)[a]

scattering	amplitude (%)	deg	path
A	100 (100)	1	$Tc_0 \rightleftarrows Tc_1$
B	63 (76)	4	$Tc_0 \rightleftarrows X_1$
C	21 (22)	4	$Tc_0 \rightleftarrows X_2$
D	7 (9)	2	$Tc_0 \rightarrow X_{1a} \rightarrow X_{1d} \leftarrow$
E	7 (9)	2	$Tc_0 \rightarrow X_{1b} \rightarrow X_{1c} \leftarrow$

[a] The amplitude (%) values in parentheses refer to $Tc_2Cl_8^{2-}$. Tc_0 represents the absorbing atoms.

infer the purity of the synthesized compounds.

EXAFS Study of $(n\text{-}Bu_4N)_2Tc_2Br_8$. The extracted EXAFS spectrum was k^2-weighted and the Fourier transformation (FT) done in the k range [3.7, 13.7] $Å^{-1}$. The phase and amplitude of the scattering function used for the adjustment were calculated using the structure of $(n\text{-}Bu_4N)_2Re_2Br_8$.[13] The amplitude of the scatterings determined in $(n\text{-}Bu_4N)_2Re_2Br_8$ permit an interpretation of the FT of $Tc_2Br_8^{2-}$ considering three single and two multiscattering wave functions. These paths involve the technetium and halogen atoms situated in the first and second shells. The amplitude and path of these large amplitude paths are presented in Table 5. In order to visualize the atoms involved in the scattering paths, a ball-and-stick representation of $Tc_2X_8^{2-}$ (X = Cl, Br) is shown in Figure 5.

The curve-fitting procedure was conducted using the five scattering wave functions determined in Table 5. In this procedure, the degeneracy, the scattering distance, and the σ^2 value of the multiscattering D and E were set equal to each other; all the other parameters were allowed to vary. The data and fit in the Fourier representation and the k^2-EXAFS spectra are shown in Figure 6. The structural parameters presented in Table 6 indicate that the first coordination shell around Tc_0 is constituted by 1(0.2) Tc atoms at 2.16(1) Å and 3.9(8) Br atoms at 2.48(1) Å. The second coordination shell is constituted by 4.3(9) Br atoms

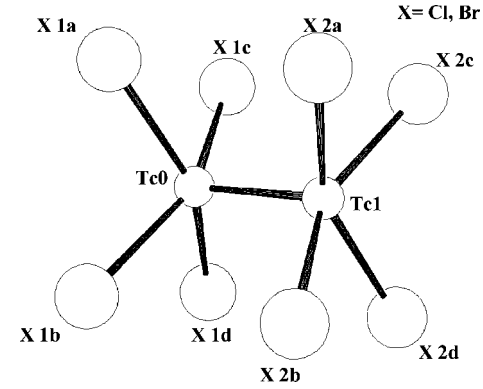

Figure 5. Ball-and-stick representation of $Tc_2X_8^{2-}$ (X = Cl, Br) in the D_{4h} geometry.

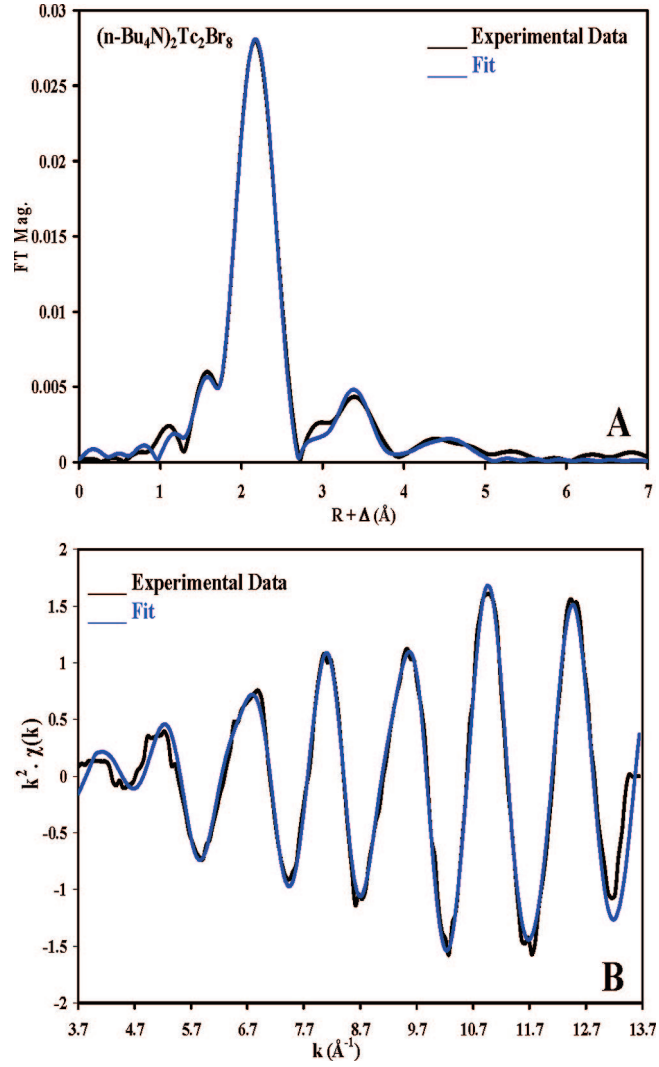

Figure 6. Fitted k^2-EXAFS spectra and Fourier transform of k^2-EXAFS spectra of $(n\text{-}Bu_4N)_2Tc_2Br_8$. Adjustment between k = [3.7, 13.7] $Å^{-1}$.

at 3.70(2) Å. From the previous results, the distance between the Br_{1a} and Br_{1d} atoms ($dBr_{1a}-Br_{1d}$) is calculated from the relation $dBr_{1a}-Br_{1d} = 2[d(Tc_0 \rightarrow Br_{1a} \rightarrow Br_{1d}) - d(Tc_0-Br_1)]$ and equals 4.84(5) Å. The same distance is found between the atoms Br_{1b} and Br_{1c}. The value $d(Tc_0 \rightarrow Br_{1a} \rightarrow Br_{1d})$ corresponds to the scattering distance of the D path (4.90 Å).

Table 6. Structural Parameter Obtained by Adjustment of the k^2-EXAFS Spectra of $(n\text{-}Bu_4N)_2Tc_2Br_8$[a]

scattering	C·N	R (Å)	σ^2 (Å^2)
$Tc_0 \rightleftarrows T\ c_1$	1(0.2)	2.16(1)	0.0026
$Tc_0 \rightleftarrows Br_1$	3.9(8)	2.48(1)	0.0023
$Tc_0 \rightleftarrows Br_2$	4.3(9)	3.70(3)	0.0087
D	2(4)	4.90(4)	0.0028
E	2(4)	4.90(4)	0.0028

[a] Adjustment between k = [3.7, 13.7] Å^{-1}. ΔE_0 = 8.1 eV.

Angular data can also be extracted from the EXAFS analysis. The average angles $Br_{1a}-Tc_0-Br_{1d}$ and $Tc_1-Tc_0-Br_1$ are derived from the relation $\cos(Br_{1a}-Tc_0-Br_{1d}) = [2d(Tc_0-Br_1)^2 - d(Br_{1a}-Br_{1d})^2]/[2d(Tc_0-Br_1)^2]$ and $\cos(Tc_1-Tc_0-Br_1) = [d(Tc_1-Tc_0)^2 + d(Tc_0\text{-}Br_1)^2 - d(Tc_1-Br_1)^2]/[2d(Tc_0-Br_1)\cdot d(Tc_0-Tc_1)]$. Calculations permit estimation of the $Br_{1a}-Tc_0-Br_{1d}$ angle to 154.74 ° and the $Tc_1-Tc_0-Br_1$ angle to 105.54°. An angle the same as $Br_{1a}-Tc_0-Br_{1d}$ is found for $Br_{1b}-Tc_0-Br_{1c}$.

EXAFS Study of $(n\text{-}Bu_4N)_2Tc_2Cl_8$. The extracted EXAFS spectra were k^2-weighted and the FT done in the k range [3.7, 13.7] Å^{-1}. The phase and amplitude function used for the adjustment were calculated using the structure of $(n\text{-}Bu_4N)_2Tc_2Cl_8$.[2] The procedure used for adjustment of the EXAFS spectra of $Tc_2Cl_8^{2-}$ is similar to the one previously used for $Tc_2Br_8^{2-}$ and involves the same type of scattering. The fitted Fourier transform and k^2-EXAFS spectra are shown in Figure 7. The structural parameters presented in Table 7 indicate that the first coordination shell around Tc_0 is constituted by 0.9(2) Tc atoms at 2.17(1) Å and 4.1(8) Cl atoms at 2.34(1) Å and the second coordination shell by 3.7(7) Cl atoms at 3.58(2) Å. Using the same approach for $Tc_2Br_8^{2-}$, the distance between Cl_{1a} and Cl_{1d} was determined to be 4.56(5) Å, the $Cl_{1a}-Tc_0-Cl_{1d}$ angle was estimated to be 153.99°, and the $Tc_1-Tc_0-Cl_1$ angle was estimated to be 105.77°.

Discussion

Synthesis of Tc(III) Dimers. The compound $(n\text{-}Bu_4N)_2Tc_2Cl_8$ is a potential precursor to many other technetium dimers, but its synthesis has proven difficult and in some instances has been controversial, as it has been claimed by several different methods.[2–4,8] In the present work, we examined the two procedures reported by Preetz et al.[8] The first, which involves an intermediate reduction of $(n\text{-}Bu_4N)_2TcCl_6$ with two equivalents of $(n\text{-}Bu_4N)BH_4$ in dichloromethane, gave very poor yields of the desired compound, which was only identified in solution by its characteristic UV–vis bands. The preponderant species in solution (>80%) was $TcCl_6^{2-}$. The second procedure involves the reduction of $(n\text{-}Bu_4N)TcOCl_4$ with two equivalents of $(n\text{-}Bu_4N)BH_4$ in THF followed by treatment of the resultant brown intermediate with acidified acetone. $(n\text{-}Bu_4N)_2Tc_2Cl_8$ is obtained in ca. 55% overall yield based on NH_4TcO_4 (Scheme 1).

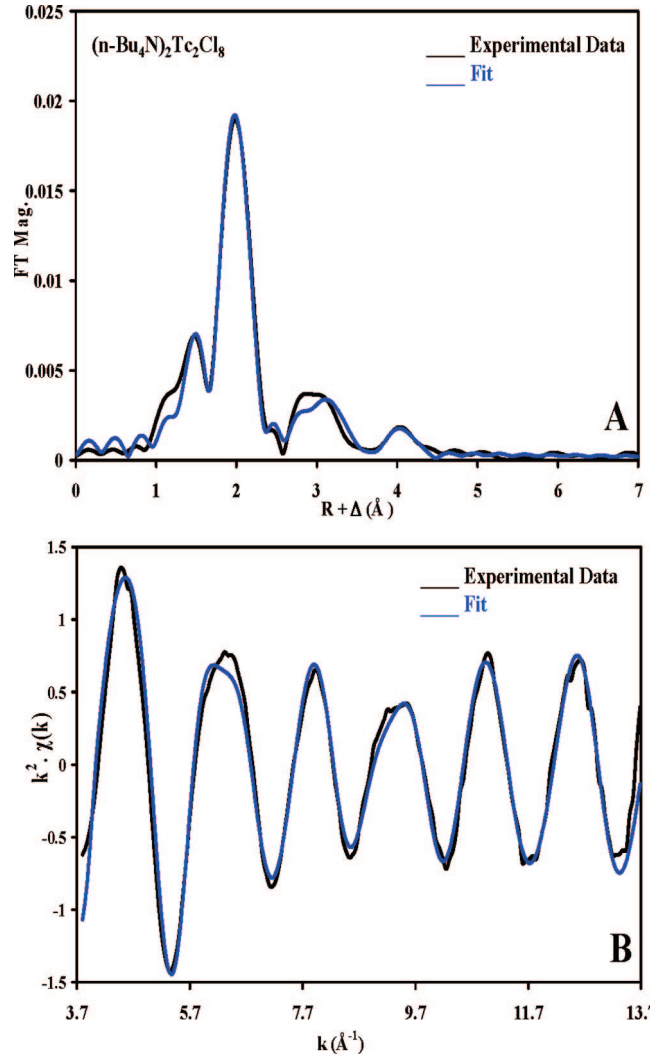

Figure 7. Fourier transform of k^2-EXAFS (A) and fitted k^2-EXAFS (B) of $(n\text{-}Bu_4N)_2Tc_2Cl_8$. Adjustment between k = [3.7, 13.7] Å^{-1}.

Table 7. Structural Parameter Obtained by Adjustment of the k^2-EXAFS Spectra of $(n\text{-}Bu_4N)_2Tc_2Cl_8$[a]

scattering	C·N	R (Å)	σ^2 (Å^2)
$Tc_0 \rightleftarrows Tc_1$	0.9(2)	2.17(1)	0.0015
$Tc_0 \rightleftarrows Cl_1$	4.1(8)	2.34(1)	0.0021
$Tc_0 \rightleftarrows Cl_2$	3.7(7)	3.58(3)	0.007
D	2.3(4)	4.62(4)	0.002
E	2.3(4)	4.62(4)	0.002

[a] Adjustment between k = [3.7, 13.7] Å^{-1}. ΔE_0 = 6.7 eV.

In both procedures, a brown solid is the product of the Tc(IV) or Tc(V) reduction with borohydride. The exact nature and structure of this compound(s) is still unknown, but its identification could give information on the mechanism of $Tc_2Cl_8^{2-}$ formation and also how to increase its yield. We were unable to isolate the brown solid in crystalline form.

EXAFS. The structural parameters determined for $M_2X_8^{2-}$ (M = Re, Tc; X = Cl, Br) by EXAFS are compared with those obtained from X-ray crystallography, estimated from Raman spectroscopy, and calculated by DFT techniques (Tables 8 and 9).[2,6–8]

For $Tc_2Br_8^{2-}$, the Tc−Tc and Tc−Br distances determined by EXAFS, 2.16(1) and 2.48(1) Å, respectively, are in

Scheme 1. Synthetic Route to $(n\text{-}Bu_4N)_2Tc_2Cl_8$.

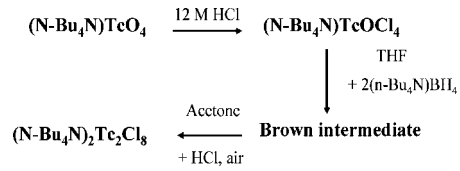

Table 8. Interatomic Distance (Å) d M−M and d M−X in $M_2X_8^{2-}$ Compound (M = Tc, Re; X = Cl, Br) Determined by EXAFS, Raman Spectroscopy, DFT, and XRD Analysis

	bond distances (M−M; M−X)			
compounds	EXAFS	DFT[6]	XRD	Raman[8]
$Tc_2Cl_8^{2-}$	(2.17; 2.34)	(2.17; 2.33)	(2.147; 2.320)[2]	
$Tc_2Br_8^{2-}$	(2.16; 2.48)	(2.18; 2.51)		(2.15; 2.47)
$Re_2Cl_8^{2-}$	(2.22; 2.36)[11]	(2.24; 2.34)	(2.222; 2.320)[27]	
$Re_2Br_8^{2-}$		(2.24; 2.51)	(2.218; 2.473)[13]	

Table 9. Average Bond Angle (deg): M−M−X and X−M−X in $M_2X_8^{2-}$ Compound (M = Tc, Re; X = Cl, Br) Determined by EXAFS, DFT, and XRD analysis[a]

	average angle (deg) M−M−X (X−M−X)		
compounds	EXAFS	DFT[6]	XRD
$Tc_2Cl_8^{2-}$	105.8 (154.0)	105	103.5 (153.1)
$Tc_2Br_8^{2-}$	105.5 (154.7)	106	
$Re_2Cl_8^{2-}$		105	103.9 (152.2)
$Re_2Br_8^{2-}$		105	103.9 (152.07)

[a] The values in parentheses refer to the trans-X−M−X angle.

agreement with the distances estimated by Raman spectroscopy, namely, 2.15 and 2.47 Å,[8] but are shorter than those calculated by DFT, namely, 2.18 and 2.51 Å.[6] For $Tc_2Cl_8^{2-}$, the Tc−Tc (2.17(1) Å) and Tc−Cl (2.34(1) Å) distances measured are slightly longer than those reported by XRD (2.147(4) Å and 2.32(2) Å, respectively). Comparison with DFT indicates that the Tc−Tc is identical, while the Tc−Cl is slightly larger. The angular data obtained by EXAFS indicate that the Tc−Tc−Br (105.5°) and Tc−Tc−Cl (105.8°) bond angles are comparable to the ones determined by DFT calculation, namely, 106° and 105°. The Tc−Tc−Cl angle measured by XRD is 103.5°.

Previous XRD studies have shown that $Tc_2Cl_8^{2-}$, $Re_2Cl_8^{2-}$, and $Re_2Br_8^{2-}$ are isostructural.[2,13] From the EXAFS results, the close similarity of the structural parameters in $Tc_2X_8^{2-}$ (X = Cl, Br; Tables 8 and 9) indicates that these compounds are also isostructural. In these two compounds, the nature of the X ligand has a negligible influence on the metal−metal separation.

Analysis of structural parameters in the $M_2Cl_8^{n-}$ complexes (M = W, Mo for $n = 4$; Tc, Re for $n = 2$) indicates that the M−M bond distances decrease moving from the sixth to the fifth period. A variation of ca. −0.08 Å is observed going from $Re_2Cl_8^{2-}$ to $Tc_2Cl_8^{2-}$, and ca. −0.12 Å from $W_2Cl_8^{4-}$ (W−W = 2.256 Å) to $Mo_2Cl_8^{4-}$ (Mo−Mo = 2.134–2.150 Å).[17] In this context, a decrease of 0.05 Å in M−M moving from $Re_2Br_8^{2-}$ to $Tc_2Br_8^{2-}$ seems quite reasonable.

XANES spectroscopy is commonly used for the characterization of the oxidation state of Tc species. In this context, previous studies have correlated the K-edge position (or

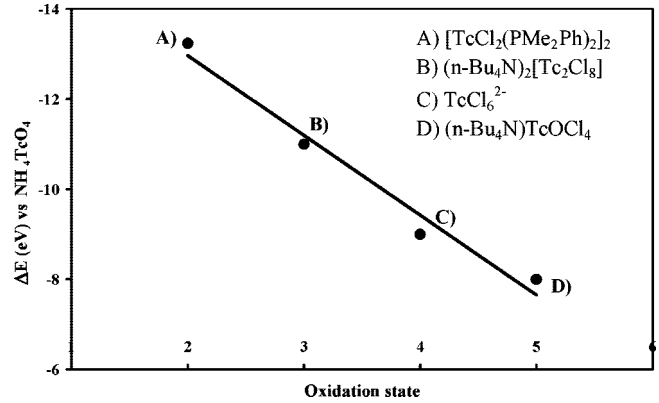

Figure 8. Chemical shift ΔE (eV) of Tc−K edge relative to NH_4TcO_4 versus formal oxidation state for (A) $[TcCl_2(PMe_2Ph)_2]_2$, (B) $(n\text{-}Bu_4N)_2Tc_2Cl_8$, (C) $TcCl_6^{2-}$, and (D) $(n\text{-}Bu_4N)TcOCl_4$.[9,18]

Table 10. Band Maxima ν (cm^{-1}) and Assignments for $Re_2Cl_8^{2-}$ [15,22] and $Tc_2Cl_8^{2-}$

Compound	ν (cm^{-1})	transition	type
$Re_2Cl_8^{2-}$	14589	$2b_{2g} \rightarrow 2b_{1ua}$	$\delta \rightarrow \delta^*$
	32003	$4e_g \rightarrow 2b_{1ua}$	$\pi(Cl) \rightarrow \delta^*$
	39447	$5e_u \rightarrow 5e_g$	$\pi \rightarrow \pi^*$
$Tc_2Cl_8^{2-}$	14713	$2b_{2g} \rightarrow 2b_{1ua}$	$\delta \rightarrow \delta^*$
	25623	$4e_g \rightarrow 2b_{1ua}$	$\pi(Cl) \rightarrow \delta^*$
	33016	$5e_u \rightarrow 5e_g$	$\pi \rightarrow \pi^*$

chemical shift ΔE) with the oxidation state (δ_{ox}) of Tc species in the following oxidation states: 0, II, IV, V, and VII; no Tc(III) species were reported.[9,10,18] A correlation between δ_{ox} and the chemical shift (ΔE) can be established for the following technetium chloro compounds: $Tc^{V}OCl_4^-$, $Tc^{IV}Cl_6^{2-}$, $Tc^{III}_2Cl_8^{2-}$, and $[Tc^{II}Cl_2(PMe_2Ph)_2]_2$. The experimental data (Figure 8) were fitted using a linear function and give the relation $\Delta E = 1.772\delta_{ox} - 16.512$ ($R^2 = 0.974$). This correlation indicated that, for a compound with $\delta_{ox} = 0$, a shift of −16.51 eV/NH_4TcO_4 is expected; this value is consistent with the one found for Tc metal, that is, −19.85 eV.[9] The relation can be used to predict the position of the K-edge absorption of other Tc chloro compounds. For example, $Tc_2Cl_8^{3-}$ has not been studied by XAFS, but a chemical shift of 12.1 eV versus TcO_4^- can be estimated.

The position of $Tc_2Br_8^{2-}$ K-edge absorption represents a shift of 1 eV to lower energy versus $Tc_2Cl_8^{2-}$. This shift could be attributed to the difference of electronegativity between Cl and Br. A recent study on Tc(IV) chloro compounds revealed a correlation between the partial charge carried by Tc and ΔE; that is, an increase of positive charge is accompanied by the shift of the K-edge absorption to higher energy.[18] Using the method previously described,[19] the partial charge on Tc in $Tc_2Br_8^{2-}$ is estimated to be +0.22 and +0.25 in $Tc_2Cl_8^{2-}$. This result is consistent with the shift observed between the two compounds.

Assignment of Electronic Transitions in the $Tc_2Cl_8^{2-}$ Optical Spectrum. A previous review[1] referenced the band at ca. 14 700 cm^{-1} in the UV–vis spectrum of $Tc_2Cl_8^{2-}$ as

(17) Cotton, F. A.; Mott, G. N.; Schrock, R. R.; Sturgeoff, L. G. *J. Am. Chem. Soc.* **1982**, *104*, 6781–6782.

(18) Poineau, F.; Fattahi, M.; Grambow, B. *Radiochim. Acta* **2006**, *94*, 559–563.

(19) Henry, M.; Jolivet, J. P.; Livage, J. *Struct. Bonding (Berlin)* **1992**, *77*, 153–206.

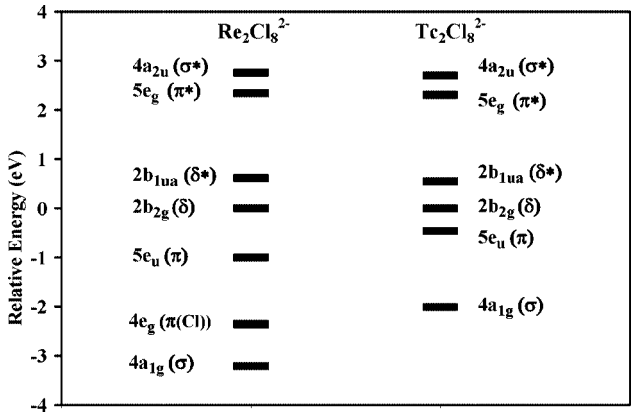

Figure 9. Calculated molecular orbital diagrams for $Re_2Cl_8^{2-}$ [21,22] and $Tc_2Cl_8^{2-}$.[23]

Table 11. Band Maxima ν (cm^{-1}) and Assignments for $Re_2Br_8^{2-}$ [15] and $Tc_2Br_8^{2-}$

compound	ν (cm^{-1})	transition	type
$Re_2Br_8^{2-}$	13957	$2b_{2g} \rightarrow 2b_{1ua}$	$\delta \rightarrow \delta^*$
	23879	$4e_g \rightarrow 2b_{1ua}$	$\pi(Br) \rightarrow \delta^*$
	26430		
	38022	$5e_u \rightarrow 5e_g$	$\pi \rightarrow \pi^*$
$Tc_2Br_8^{2-}$	13717	$2b_{2g} \rightarrow 2b_{1ua}$	$\delta \rightarrow \delta^*$
	18647	$4e_g \rightarrow 2b_{1ua}$	$\pi(Br) \rightarrow \delta^*$
	20518		
	35714	$5e_u \rightarrow 5e_g$	$\pi \rightarrow \pi^*$

the $\delta \rightarrow \delta^*$ transition. Assignments for the remaining two intense bands in the spectrum of $Tc_2Cl_8^{2-}$ have not been made. It seems reasonable, given the close similarity between the spectra of $Tc_2Cl_8^{2-}$ and $Re_2Cl_8^{2-}$ (Figure 3), to make assignments similar to those proposed for $Re_2Cl_8^{2-}$ (Table 10).[14,20–22] Examination of Table 10 indicates that the position of the $\pi \rightarrow \pi^*$ and $\pi(Cl) \rightarrow \delta^*$ transitions are shifted to higher energy for the Re compound. The relative positions of the $\delta \rightarrow \delta^*$, $\pi \rightarrow \pi^*$, and $\pi(Cl) \rightarrow \delta^*$ transitions in $M_2Cl_8^{2-}$ (M = Tc, Re) can be correlated to the electronic structure calculations on these compounds.[20–23] Approximate MO diagrams for the two compounds are shown in Figure 9.

A comparison of the MO diagrams indicates that (1) the energy separation between the δ and δ^* orbitals is nearly identical in $Tc_2Cl_8^{2-}$ and $Re_2Cl_8^{2-}$ and (2) the difference of energy between π and π^* is greater for the Re than for the Tc compound. It follows that the $\pi \rightarrow \pi^*$ transition should occur at higher energy for the rhenium compound.

Assignment of Transitions in the $Tc_2Br_8^{2-}$ Spectrum. For the first time, the UV–vis spectrum of $Tc_2Br_8^{2-}$ is reported. It exhibits four intense absorption bands and is similar to $Re_2Br_8^{2-}$ spectra. The UV–vis spectrum of $Re_2Br_8^{2-}$ has already been studied,[15,22] but only three of the four intense bands were assigned; the band around 26 000 cm^{-1} was not assigned. The similarity of the Re and Tc spectra led to the assignments proposed in Table 11.

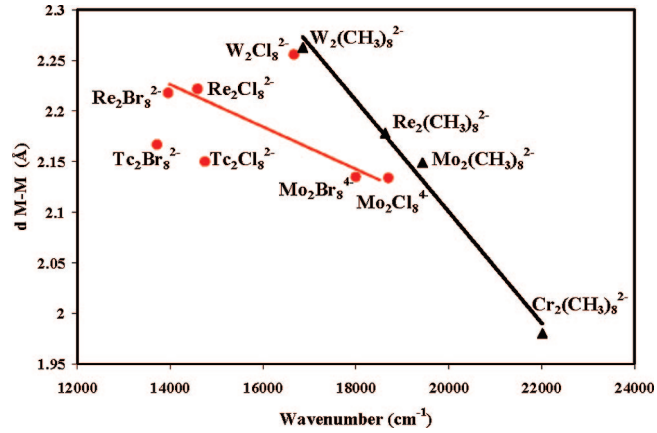

Figure 10. Atomic distance d M−M (Å) vs $\delta \rightarrow \delta^*$ transition energy (cm^{-1}) in $M_2X_8^{2-}$ (X = Cl, Br; M = Tc, Re; M = Mo, W;[17,26] in red) and in $M_2(CH_3)_8^{2-}$ (M = W, Re, Mo, Cr; in black).[24,25] The line in black is the correlation found by Sattelberger and Fackler for $M_2(CH_3)_8^{n-}$ (M = W, Re, Mo, Cr).[25] The line in red is the correlation found by Clark and D'Urso for $M_2X_8^{n-}$ (M = Mo, Re, X = Cl, Br).[26]

Study of the $\delta \rightarrow \delta^*$ Position. Previous studies on the octamethyldimetalate compounds, $M_2(CH_3)_8^{n-}$ [24,25] have shown that the position of the $\delta \rightarrow \delta^*$ transition can be correlated with the M−M distance. The observation made for M = Re, Cr, Mo, and W is that the energy of the $\delta \rightarrow \delta^*$ transition increases linearly when the distance M−M decreases (Figure 10). A similar correlation was suggested for the quadruply M−M bonded halide dimers, $M_2X_8^{n-}$ (M = Mo, Re; X = Cl, Br).[26] We have added the two technetium compounds described here and the previously reported $W_2Cl_8^{4-}$ to Figure 10. It is clear that the correlation between $\delta \rightarrow \delta^*$ and d M−M found for the $M_2(CH_3)_8^{n-}$ compounds does not extend to the $M_2X_8^{n-}$ compounds. The pπ orbitals on the halogen ligands interact to varying degrees with the δ and δ^* orbitals on the metals and influence the energy of the $\delta \rightarrow \delta^*$ transition in subtle and, at this time, unpredictable ways.

Conclusion

The compounds $(n\text{-}Bu_4N)_2Tc_2X_8$ (X = Cl, Br) were synthesized and examined by EXAFS and UV–vis spectroscopy, and the structural and spectroscopic results were compared to those of their rhenium congeners. The synthetic procedure reported here for $(n\text{-}Bu_4N)_2Tc_2Cl_8$ starting from $(n\text{-}Bu_4N)TcOCl_4$ has been reproduced several times in our laboratory. Typical yields are in the range of 65%. An alternative synthesis starting from $(n\text{-}Bu_4N)_2TcCl_6$ gave poor to negligible yields of the quadruply bonded dimer and was abandoned. A reliable synthesis for $(n\text{-}Bu_4N)_2Tc_2Cl_8$ will facilitate the synthesis of other quadruply bonded techne-

(20) Gagliardi, L.; Roos, B. O. *Inorg. Chem.* **2003**, *42*, 1599–1603.
(21) Bursten, B. E.; Cotton, F. A.; Fanwick, P. E.; Stanley, G. G. *J. Am. Chem. Soc.* **1983**, *105*, 3082–3087.
(22) Mortola, A. P.; Moskowitz, J. W.; Roesch, N.; Cowman, C. D.; Gray, H. B. *Chem. Phys. Lett.* **1975**, *32*, 283–286.
(23) Plekhanov, Yu. V.; Kryuchkov, S. V. *Radiochem. (Engl. Trans.)* **1997**, *39*, 208–212.
(24) Ferrante, F.; Gagliardi, L.; Bursten, B. E.; Sattelberger, A. P. *Inorg. Chem.* **2005**, *44*, 8476–8480.
(25) Sattelberger, A. P.; Fackler, J. P. *J. Am. Chem. Soc.* **1977**, *99*, 1258–1259.
(26) Clark, R. J.; D'Urso, N. R. *J. Am. Chem. Soc.* **1978**, *100*, 3088–3091.
(27) Cotton, F. A.; Frenz, B. A.; Stults, B. R.; Webb, R. *J. Am. Chem. Soc.* **1976**, *98*, 2768–2773.

tium(III) dimers, for example, $Tc_2(O_2CR)_4X_2$, $[Tc_2(CH_3)_8]^{2-}$, $Tc_2Cl_6(PR_3)_2$, and so forth. This work is in progress in our laboratory and will be reported in due course.[28]

Our EXAFS analyses of $Tc_2X_8^{2-}$ provided structural parameters that are in excellent agreement with the recent DFT calculations of Kaltsoyannis and Cavigliasso and infer the isostructural nature of these species.[6,7] The similarity of the optical spectra and electronic structures of analogous Re and Tc compounds permits the assignment of several previously unassigned transitions in the $Tc_2X_8^{2-}$ spectra. Of particular note is the near coincidence of the $\delta \rightarrow \delta^*$ transitions in $M_2Cl_8^{2-}$ and $M_2Br_8^{2-}$ (M = Tc, Re). Additional theoretical analysis of the electronic transitions in $M_2X_8^{n-}$ compounds will be needed to explain why this is the case for Tc/Re pairs but not for Mo/W pairs.

(28) Poineau, F.; Sattelberger, A. P.; Czerwinski, K. *J. Coord. Chem.* In press.

Acknowledgment. The authors are grateful to Dr. Carol J. Burns (Los Alamos) for a generous loan of ammonium pertechnetate. The authors thank Efrain E. Rodriguez (Los Alamos) for fruitful discussions on X-ray diffraction, and Prof. Laura Gagliardi (University of Geneva) for discussions on the electronic structure of quadruply metal–metal bonded complexes. We also acknowledge support from the Los Alamos Laboratory Directed Research and Development (LDRD) program for partial support of this work. This work was supported by the U.S. Department of Energy, agreement no. DE-FG07-01AL67358.

IC701453K